Bistability-Mediated Carrier Recombination at Light-Induced Boron-Oxygen Complexes in Silicon

Mao-Hua Du, Howard M. Branz, Richard S. Crandall, and S. B. Zhang
National Renewable Energy Laboratory, Golden, Colorado 80401, USA
(Received 18 July 2005; published 22 December 2006)

A first-principles study of the BO_2 complex in B-doped Czochralski Si reveals a defect-bistability-mediated carrier recombination mechanism, which contrasts with the standard fixed-level Shockley-Read-Hall model of recombination. An O_2 dimer distant from B causes only weak carrier recombination, which nevertheless drives O_2 diffusion under light to form the BO_2 complex. Although BO_2 and O_2 produce nearly identical defect levels in the band gap, the recombination at BO_2 is substantially faster than at O_2 because the charge state of the latter inhibits the hole capture step of recombination.

DOI: 10.1103/PhysRevLett.97.256602 PACS numbers: 72.20.Jv, 61.72.Bb, 61.72.Ji, 71.55.Cn

Nonradiative carrier recombination at defects can limit photovoltaic and luminescent device efficiencies; a better understanding of recombination-active defects and recombination mechanisms will be vital to future device improvements. Deep level transient spectroscopy is often used to detect semiconductor deep levels, and the Shockley-Read-Hall (SRH) theory [1,2], which assumes carrier recombination at fixed energy levels, is used to calculate recombination rates. While the SRH theory has been quite successful for more than a half century, there is no *a priori* reason to accept the assumption that defect energy levels are fixed during the recombination. In fact, many known defects exhibit strong electron-phonon coupling, resulting in carrier-trapping-induced defect structure relaxation that can influence recombination rates significantly.

We studied carrier recombination in a defect that limits the efficiency of solar cells made on B-doped Czochralski silicon (Cz-Si) wafers. These cells can lose up to 10% of their initial energy-conversion efficiency due to illumination-induced formation of recombination centers [3]. Similar degradation was observed by minority carrier injection [4]. Since Cz-Si typically has high oxygen concentration $[O] \sim 10^{17}$–10^{18} cm^{-3}, the origin of the degradation is attributed to a B and O complex [5–7]. The linear dependence of the complex density upon both [B] and $[O]^2$ further suggests that the complex is BO_2 [7,8]. Schmidt and Bothe proposed that the interstitial oxygen dimers diffuse to B to form the BO_2 centers [7,8] but left at least three fundamental questions that must be addressed: (i) How do electrons and holes (e^- and h^+) recombine through the BO_2 complex? (ii) Why is the BO_2 complex a more effective recombination center than the uncomplexed O_2 dimer? (iii) What explains the observed light-induced BO_2 formation kinetics?

The oxygen dimer has an unusual bistability, between a square (sq) and a staggered (st) configuration: Alternation between these configurations can lead to O_2 diffusion [9–11]. Adey *et al.* showed that illumination can cause charge state change that drives O_2 diffusion, and this can lead to O_2 trapping at substitutional B [9]. They also calculated the annealing energy of the BO_2 complex, in agreement with the experimental value. However, Ref. [9] did not point out that the O_2 diffusion process itself is a recombination process. Furthermore, their fixed-gap-level recombination model for the BO_2 complex is invalid because (i) the defect levels introduced by BO_2 and O_2 are nearly identical (see Fig. 1), as revealed by our first-principles calculations [12], so their model does not solve the critical problem of why the BO_2 is a strong recombination center but the uncomplexed O_2 is not; and (ii) the calculated defect level is only about 0.2 eV below the conduction band edge and may be too shallow to act as an effective recombination center in the SRH theory.

In this Letter, we show that both BO_2 and O_2 are recombination centers in which recombination is mediated by large lattice relaxation upon carrier trapping. However,

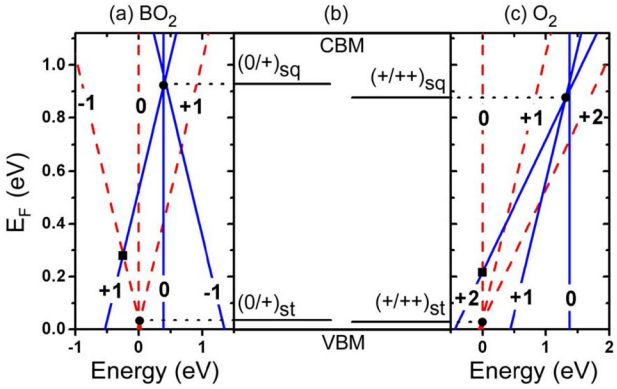

FIG. 1 (color online). Energies of (a) BO_2 and (c) uncomplexed O_2 in the square (solid blue lines) and staggered (dashed red lines) configurations as functions of the Fermi level (E_F). Energies for the charge-neutral staggered configurations are set to zero. Horizontal solid lines in the central panel (b) emphasize the similarities between the two defects: The transition energies in each defect are nearly identical for both sq and st configurations. The location of E_F at the ground-state transition of each defect is indicated by the squares.

the presence of uncomplexed O_2 in silicon does not cause a significant reduction of the carrier lifetime because h^+ trapping by the positively charged $O_2{}^+$ is slowed by Coulomb repulsion, and this majority carrier capture process limits the carrier recombination rate. The binding of B to O_2 changes the net charge at the defect complex and dramatically increases the h^+ capture and recombination rates. Our work provides a simple explanation of the enhanced recombination due to the binding of O_2 with B, as well as improved understanding of light-induced O_2 diffusion. The slow h^+ trapping at O_2 also explains the observed defect generation rate dependence on [B] and the saturation of the rate at relatively low-illumination intensity.

Our calculations are based on the density functional theory within the local density approximation, as implemented in the VASP codes [13]. The electron-ion interactions are described by ultrasoft pseudopotentials [14]. The valence wave functions are expanded in a plane-wave basis with a cutoff energy of 300 eV. We have used a $2 \times 2 \times 2$ k-point mesh and a 216-atom supercell to calculate the total energy and a 64-atom cell to calculate the energy barrier using a nudged elastic band method [15]. Atoms are relaxed until the forces are less than 0.02 eV/Å.

Figures 2(a) and 2(b) show the ground-state structures of the sq and st BO_2 complexes, obtained by a systematic search up to third-nearest neighbors between B and O_2 [16]. Our calculated ground-state BO_2 structures agree with West *et al.* [17] but not with Adey *et al.* [9], who placed B at the nearest oxygen-neighbor site labeled X. Because of the local ionicity induced by highly electronegative O, the Si at site X (Si_X) is positively charged, while its two neighboring O atoms and the B acceptor are all negatively charged. As a result, the second-nearest-neighbor binding of B to O_2 [see Figs. 2(a) and 2(b)] is more favored than the nearest-neighbor binding, because of the Si_X-O_2 and Si_X-B Coulomb attraction and the reduced B-O Coulomb repulsion. Figure 1(a) shows that the ground states of BO_2 are $BO_2^{sq,+}$ and $BO_2^{st,-}$ depending on the Fermi level. For these two configurations, our calculations show that the second-nearest-neighbor binding of B is more stable than the nearest-neighbor binding by 0.24 and 0.26 eV, respectively. Figure 1(c) shows that the ground states of O_2 are $O_2^{sq,++}$ and $O_2^{st,0}$. The binding with B has little effect on the structure of O_2. It only adds the $(-)$ charge of B to the defect complex. The transition between $BO_2^{sq,+}$ and $BO_2^{st,-}$ (at $E_v + 0.29$ eV, where E_v is valence band-edge energy) is also only slightly different from that between $O_2^{sq,++}$ and $O_2^{st,0}$ (at $E_v + 0.22$ eV). We have calculated the binding energy between B^- and $O_2^{sq,++}$ and $O_2^{st,0}$ to be 0.55 and 0.42 eV, respectively.

Since the boron-doped Si is p-type, the BO_2 ground state is thus $BO_2^{sq,+}$ as shown in Fig. 1(a). Our calculation shows a 0.82-eV barrier for the $BO_2^{sq,+} \rightarrow BO_2^{st,+}$ transition, so sq $\rightarrow$ st reconfiguration is unlikely in the dark. Under light,

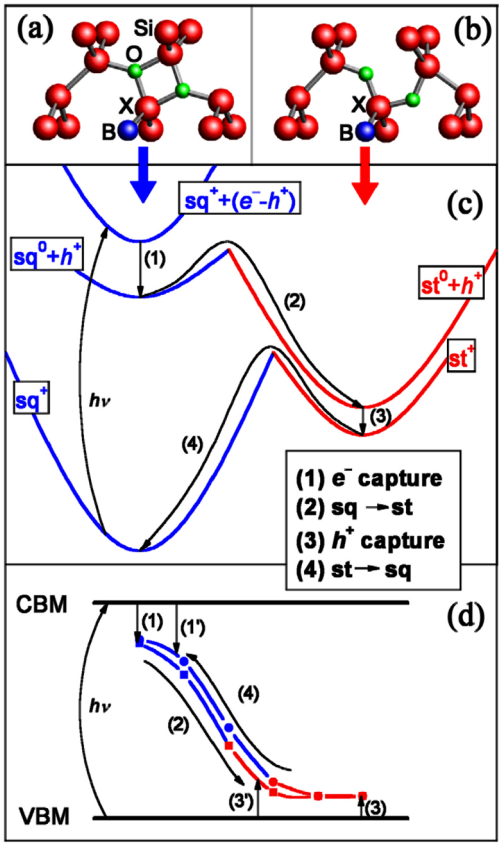

FIG. 2 (color online). Diagrams of the lowest energy B binding sites in both the (a) square and (b) staggered BO_2 complex are above the corresponding configurations of (c) and (d). (c) shows a schematic configuration-coordinate total energy diagram for recombination. The solid arrows indicate the recombination steps (1)–(4). The arrow marked $h\nu$ indicates band-to-band electronic excitation. (d) shows single-particle electronic-level positions during the recombination. Here squares (circles) represent electron (hole) occupied levels on step (2) [(4)]. The arrows labeled (1′) and (3′) indicate partial-reconfiguration e^- and h^+-capture steps. Uncomplexed O_2 diagrams are nearly identical, except for the increase of net charge by 1.

however, sq $\leftrightarrows$ st reconfiguration can take place in an efficient way, with recombination assisted by reconfiguration as follows:

$$(1)\ BO_2^{sq,+} + e^- \longrightarrow BO_2^{sq,0},$$

$$(2)\ BO_2^{sq,0} \xrightarrow{\text{reconfig}} BO_2^{st,0},$$

$$(3)\ BO_2^{st,0} + h^+ \longrightarrow BO_2^{st,+},$$

$$(4)\ BO_2^{st,+} \xrightarrow{\text{reconfig}} BO_2^{sq,+}.$$

The numbered processes here are also represented by the corresponding numbered solid arrows in Figs. 2(c) and 2(d). Step (1) is an e^- trapping to a level at $E_c - 0.2$ eV. Step (2) is a reconfiguration process,

which causes a shallow-to-deep transition of the filled electron level, as shown in Fig. 2(d). The 0.2-eV energy emitted in step (1) may assist the conversion of $BO_2^{sq,0}$ to $BO_2^{st,0}$ over the 0.17-eV barrier in step (2) [18]. Step (3) is an h^+ trapping to a level at $E_v + 0.02$ eV. In analogy to step (2), the reconfiguration in step (4) causes a shallow-to-deep transition of the hole-occupied level, as shown in Fig. 2(d). Through the sq $\leftrightarrows$ st reconfigurations of steps (1)–(4), the energy of an $(e^-$-$h^+)$ pair is released to lattice vibrations (or phonons). Although the BO_2 continually flips back and forth between the sq and st configurations induced by carrier trapping, most O_2 do not easily diffuse away from the B, because of the 0.5-eV binding energy.

Note that the above discussion applies when the carrier concentration is low. When the concentration is higher, recombination may not have to complete steps (2) and (4). For instance, a hole, the majority carrier, may be captured at (3′) in Fig. 2(d) before step (2) is completed. This is particularly true for the BO_2^0 complex, which has a permanent multipole moment that attracts holes to the negatively charged O and B ends (in contrast to spherically symmetric neutral point defects which must rely on induced dipoles to trap carriers). Similarly, an electron may be captured at (1′) before step (4) is completed. These alternative paths should have significantly reduced emission probabilities for the captured carriers and reduced (or even eliminated) energy barriers for the sq $\leftrightarrows$ st reconfigurations [cf. Fig. 2(c)]. Clearly, the standard SRH analysis [6,19] with its fixed level assumption will need to be reevaluated for such defect-relaxation-mediated recombination where the defect level sweeps up and down within the band gap.

The sq $\leftrightarrows$ st reconfigurations of an uncomplexed O_2 have nearly identical barriers as the BO_2 in Fig. 2(c). One may therefore naively assume that the same e^--h^+ recombination mechanism should also apply to the uncomplexed O_2. However, without the associated B^-, h^+ trapping to the positively charged O_2^+ must now overcome a repulsive capture barrier. It has been demonstrated that Coulomb repulsion normally decreases the capture probability by orders of magnitude [20]. This results in slow recombination which is not expected to affect the minority carrier lifetime.

The O_2 diffusion path is illustrated in Fig. 3. Carrier-recombination-assisted reconfigurations can take place as follows:

$$\text{(1)}\ O_2^{sq,++} + e^- \longrightarrow O_2^{sq,+},$$

$$\text{(2)}\ O_2^{sq,+} \xrightarrow{\text{reconfig}} O_2^{st,+},$$

$$\text{(R)}\ O_2^{st,+} \xrightarrow{\text{O rotation}} O_2^{st,+},$$

$$\text{(3)}\ O_2^{st,+} + h^+ \longrightarrow O_2^{st,++}\ \text{(slow)},$$

$$\text{(4)}\ O_2^{st,++} \xrightarrow{\text{reconfig}} O_2^{sq,++}.$$

While steps (1)–(4) here each have their own BO_2 counterpart, in order for the O_2 to diffuse away, however, one additional step, namely, step (R), is required. In step (R), which connects the configuration of Figs. 3(b) and 3(c), the O atoms on the bridge sites rotate over a small barrier of 0.1 eV [10]. The bottleneck of the O_2 diffusivity is step (3), which is slow due to the repulsive h^+-capture barrier described above. This slow recombination-driven diffusion process is consistent with the observed low BO_2 defect generation rate [8].

The BO_2 generation rate should depend on [B], $[O_2]$, and the O_2 hop rate. The hop rate is proportional to the e^--h^+ recombination rate $1/\tau$, where τ is the time for O_2 to complete one recombination cycle. Therefore, the BO_2 defect generation rate is $R_{gen} \propto [B][O_2]/\tau$ [21]. By examining which carrier (e^- or h^+) is rate-limiting for recombination under different experimental conditions, the dependences of R_{gen} on [B] and illumination intensity I can be predicted. Table I shows the asymptotic forms predicted at both high and low intensities and also lists the corresponding experimental literature. The fact that all of our predictions agree with experiment gives strong support to our suggestion that carrier recombination drives the O_2 diffusion. In particular, the slow h^+-trapping rate limits the O_2 diffusion at high intensity (e.g., at typical solar illumination intensities), and, thus, the BO_2 generation rate is independent of I. Only in the low-illumination intensity regime where I is less than about 1 mW/cm^2 does the minority e^- capture become so slow that it limits the recombination rate. Our theory also predicts, at low-illumination intensity, $R_{gen} \propto [B]$, which to our knowledge has not been tested.

Finally, we consider the effects of the larger group III acceptor atoms in Cz-Si, e.g., Ga. In contrast to B, which

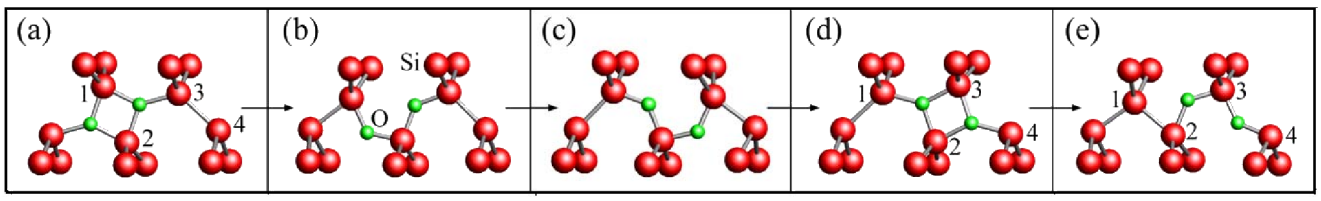

FIG. 3 (color online). Oxygen dimer diffusion pathway along {110}. (a)–(d) show key steps on the oxygen dimer pathway as it moves from between Si atoms 1 and 2 to between Si atoms 2 and 3. (e) shows the first step in moving the dimer further to between Si atoms 3 and 4.

TABLE I. Rate-limiting process (RLP) in recombination-driven diffusion of O_2, O_2 hop rate, and the resulting defect generation rate (R_{gen}) at high- and low-illumination intensity (I). Experimental references are shown in parentheses and agree with our theoretical predictions. τ_{cn} and τ_{cp} are e^- and h^+ capture time constants, and c_n and c_p are e^- and h^+ capture rate coefficients, respectively.

I	RLP	Hop rate	$R_{gen} \propto [B]/\tau$
High	h^+ trapping	$1/\tau \approx 1/\tau_{cp} = c_p[p] \propto [B]$	$R_{gen} \propto [B]^2$ (Ref. [22]); independent of I (Ref. [5])
Low	e^- trapping	$1/\tau \approx 1/\tau_{cn} = c_n[n] \propto I$	$R_{gen} \propto [B]$; $R_{gen} \propto I$ (Ref. [5])

binds both O_2^{sq} and O_2^{st}, we find that Ga binds only the O_2^{sq} but repels the O_2^{st}. Our analysis shows that the larger substitutional Ga puts the Si lattice into local compressive strain, which is compatible with the local tensile strain of Si around O_2^{sq} but incompatible with the compressive strain induced by O_2^{st} along the Si zigzag chains. This incompatibility blocks the O_2 diffusion pathway shown in Fig. 3, as the sq → st reconfiguration from Figs. 3(a) and 3(b) becomes energetically unfavorable. This prevents the formation of the GaO_2 complex and explains why the coexistence of O and Ga does not cause the kind of light-induced degradation observed when O and B coexist [7]. Degradation would also clearly not be expected for In and other large acceptor atoms in Cz-Si.

In summary, we propose a bistability-mediated recombination mechanism for BO_2 in Cz-Si. Such a carrier-trapping-induced defect relaxation process, accompanied by changes in the defect level positions, may also take place at other defect complexes in semiconductors. The standard fixed-level Shockley-Read-Hall theory must be applied with great caution to such cases. We also explain how a change of the net defect charge state drastically increases the carrier recombination rate at BO_2 compared to the rate at O_2. Although the uncomplexed O_2 must act as a recombination center in order to diffuse, the Coulomb barrier to h^+ trapping at the O_2^+ means that the minority carrier lifetime should not be affected until the BO_2 complex forms. This recombination-driven O_2 diffusion model is supported by a number of experimental observations including the defect generation rate dependences on [B] and on the illumination intensity.

We thank Sukit Limpijumnong and Tihu Wang for helpful discussions. This work was supported by the U.S. Department of Energy, BES and EERE, under Contract No. DE-AC39-98-GO10337.

[1] W. Shockley and W. T. J. Read, Phys. Rev. **87**, 835 (1952).
[2] R. N. Hall, Phys. Rev. **87**, 387 (1952).
[3] H. Fischer and W. Pschunder, in *Proceedings of the Tenth IEEE Photovoltaic Specialists Conference* (IEEE, New York, 1973), p. 405.
[4] J. Knobloch, S. W. Glunz, D. Biro, W. Warta, E. Schaffer, and W. Wettling, in *Proceedings of the 2nd IEEE Photovoltaic Specialists Conference* (IEEE, New York, 1996), p. 404.
[5] J. Schmidt, A. G. Aberle, and R. Hezel, in *Proceedings of the 26th IEEE Photovoltaic Specialists Conference* (IEEE, New York, 1997), p. 13.
[6] J. Schmidt and A. Cuevas, J. Appl. Phys. **86**, 3175 (1999).
[7] J. Schmidt and K. Bothe, Phys. Rev. B **69**, 024107 (2004).
[8] K. Bothe, R. Hezel, and J. Schmidt, Solid State Phenom. **95–96**, 223 (2004).
[9] J. Adey, R. Jones, D. W. Palmer, P. R. Briddon, and S. Oberg, Phys. Rev. Lett. **93**, 055504 (2004).
[10] Y. J. Lee, J. von Boehm, M. Pesola, and R. M. Nieminen, Phys. Rev. Lett. **86**, 3060 (2001).
[11] Y. J. Lee, J. von Boehm, M. Pesola, and R. M. Nieminen, Phys. Rev. B **65**, 085205 (2002).
[12] Formation energies are calculated according to S. B. Zhang, J. Phys. Condens. Matter **14**, R881 (2002).
[13] G. Kresse and J. Furthmuller, Phys. Rev. B **54**, 11 169 (1996).
[14] D. Vanderbilt, Phys. Rev. B **41**, R7892 (1990).
[15] G. Henkelman and H. Jónsson, J. Chem. Phys. **113**, 9978 (2000), and references therein.
[16] See EPAPS Document No. E-PRLTAO-97-018652 for supplementary materials. For more information on EPAPS, see http://www.aip.org/pubservs/epaps.html.
[17] D. West, M. Sanati, and S. K. Estreicher, Phys. Rev. B **72**, 165206 (2005).
[18] We find a lower barrier for the $BO_2^{sq,0} \rightarrow BO_2^{st,0}$ reconfiguration than the 0.78-eV barrier reported in Ref. [9]. Therefore, the BO_2 is not trapped in the sq configuration as predicted there.
[19] S. Rein and S. W. Glunz, Appl. Phys. Lett. **82**, 1054 (2003).
[20] *Electronic Materials Science: For Integrated Circuits in Si and GaAs*, edited by J. W. Mayer and S. S. Lau (MacMillan, New York, 1990).
[21] The derivation of $R_{gen} \propto [O_2^{sq,++}]$ given in Ref. [9] is invalid. The generation rate should depend on the total $[O_2]$, rather than $[O_2^{sq,++}]$, because O_2 diffusion can start either from $O_2^{sq,++}$ by e^- trapping or from $O_2^{st,0}$ by h^+ trapping.
[22] S. Rein, T. Rehrl, W. Warta, S. W. Glunz, and G. Willeke, in *Proceedings of the 17th European Photovoltaic Solar Energy Conference* (WIP-ETA, Munich, 2001), p. 1555.